Immunity to infection

Clinical

Short Communication

Discriminating promiscuous from target-specific autoantibodies in COVID-19

*Mikhail Lebedin[1,2], Clara Vázquez García[1,2], Lisa Spatt[1],
Christoph Ratswohl[1], Charlotte Thibeault[2], Lennard Ostendorf[3],
Tobias Alexander[4,5], Friedemann Paul[2], Leif Erik Sander[2,6],
Florian Kurth[2] and Kathrin de la Rosa[1,6]*

[1] Max Delbrück Center for Molecular Medicine in the Helmholtz Association, Berlin, Germany
[2] Charité – Universitätsmedizin Berlin, Corporate Member of Freie Universität Berlin and Humboldt-Universität zu Berlin, Berlin, Germany
[3] Department of Nephrology and Medical Intensive Care Medicine, Charité – Universitätsmedizin Berlin, Corporate Member of Freie Universität Berlin and Humboldt-Universität zu Berlin, Berlin, Germany
[4] Department of Rheumatology and Clinical Immunology, Charité – Universitätsmedizin Berlin, Corporate Member of Freie Universität Berlin and Humboldt-Universität zu Berlin, Berlin, Germany
[5] Deutsches Rheumaforschungszentrum (DRFZ Berlin) – a Leibniz Institute, Berlin, Germany
[6] Berlin Institute of Health (BIH) at Charité, Berlin, Germany

Diverse autoantibodies were suggested to contribute to severe outcomes of COVID-19, but their functional implications are largely unclear. ACE2, the SARS-CoV-2 receptor and a key regulator of blood pressure, was described to be one of many targets of autoantibodies in COVID-19. ACE2 in its soluble form (sACE2) is highly elevated in the blood of critically ill patients, raising the question of whether sACE2:spike complexes induce ACE2 reactivity. Screening 247 COVID-19 patients, we observed elevated sACE2 and anti-ACE2 IgG that were poorly correlated. Interestingly, levels of IgGs recognizing ACE2, IFNα2, and CD26 strongly correlated in severe COVID-19, with 15% of sera showing polyreactivity versus 4.1% exhibiting target-directed autoimmunity. Promiscuous autoantibodies failed to impair the activity of ACE2 and IFNα2, while only specific anti-IFNα2 IgG compromised cytokine function. Our study suggests that the detection of autoantibodies in COVID-19 is often attributed to a promiscuous reactivity, potentially misinterpreted as target-specific autoimmunity with functional impact.

Additional supporting information may be found online in the Supporting Information section at the end of the article.

Correspondence: Prof. Kathrin de la Rosa
e-mail: Kathrin.delaRosa@mdc-berlin.de

Introduction

Severe acute respiratory syndrome coronavirus 2 (SARS-CoV-2) infections can be asymptomatic or manifest in coronavirus disease 2019 (COVID-19) with mild to severe, as well as long-lasting

symptoms. Pre-existing autoantibodies that neutralize type 1 interferons were suggested to increase the risk of severe COVID-19 [1], representing a potentially predictive biomarker with direct implications for medical treatment. Other studies described anti-phospholipid autoantibodies and a causal link to thrombosis in COVID-19, or anti-heart antibodies that were correlated with clinical symptoms [2–4]. High-throughput autoantibody discovery platforms unraveled that COVID-19 patients have a high prevalence of self-reactive antibodies against diverse immunomodulatory proteins that perturb immune function [5]. A similar study showed that about 80% of COVID-19 patients develop autoantibodies recognizing secreted or cell surface antigens [6]. A broad literature review on self-reactive antibodies and autoimmune manifestations in COVID-19 summarizes a total of 17 different autoantibody targets and 15 autoimmune diseases associated with SARS-CoV-2 infections [7]. Causal links between autoantibodies and COVID-19 pathogenesis need, however, careful evaluation and depend on the affinity, specificity, and longevity of the antibodies.

Angiotensin-converting enzyme 2 (ACE2), the high-affinity receptor for SARS-CoV-2 [8], was reported to be a target of autoantibodies that potentially contribute to COVID-19 pathogenesis via antibody-mediated inhibition of ACE2 enzymatic activity [9–11]. ACE2 has several physiological functions including regulation of blood pressure [12] and inflammation [13], which were shown to protect mice from acute lung injury [14]. The membrane-bound form of the ACE2 receptor is cleaved by a disintegrin and metalloprotease 17 (ADAM17) [15] and transmembrane protease serine subtype 2 (TMPRSS2) [16]. Soluble ACE2 (sACE2) is increased in the blood of COVID-19 patients and correlates with disease severity [17]. However, the contribution of sACE2 to autoimmunity, as well as the functional consequences of anti-ACE2 immunoglobulin (Ig) in COVID-19 pathogenesis, is rather obscure.

Results and discussion

Anti-ACE2 autoantibodies in COVID-19 are unlikely to result from high concentration of soluble ACE2

To measure titers of ACE2-reactive IgG, serial dilutions of 640 serum samples from 247 COVID-19 patients and 96 serum samples from 96 healthy donors were tested by ELISA. COVID-19 patients were stratified according to the World Health Organization (WHO) ordinal scale ranging from WHO1–2 for outpatients, WHO3–5 for moderate cases, WHO6–7 for a severe disease course with need for invasive mechanical ventilation, and 8 for patients who died [18]. Patients and healthy donors were not vaccinated, as samples were collected during the first COVID-19 wave. Overall, anti-ACE2 IgG titers observed in patients were very low in comparison to anti-SARS-CoV-2 RBD titers, likely reflecting modest auto-antibody affinity and concentration (Fig. 1A). However, anti-ACE2 IgG was significantly higher in moderate and severe COVID-19 (2.34-fold increase for WHO3-5 and 4.24-fold

increase for WHO6+ patients in comparison to healthy donors, Fig. 1B). Anti-ACE2 IgG levels peaked during the acute phase of the disease at 25 days post symptom onset and persisted for up to 2 months in some individuals (Fig. 1C). The level of ACE2-reactive IgG was increased 1.57-fold for female compared to male patients and 1.75-fold for patients above the age of 45 within the severe COVID-19 cases (Supporting information Fig. S1A and B). The titers of anti-ACE2 IgG rarely exceeded an ED50 (effective dilution 50; effective serum dilution at which half of specific IgG is bound) of 100. By contrast, the level of anti-SARS-CoV-2 RBD IgG was two orders of magnitude higher (median ED50 anti-ACE2: 5.35; median ED50 anti-RBD 573.7; Fig. 1D and E). Anti-ACE2 IgG levels did not show a strong correlation with anti-RBD IgG, suggesting that the degree of ACE2-directed autoimmunity is independent of the immune response against the pathogen (Fig. 1F).

If sACE2 were recruited into the GC response through the formation of sACE2:spike complexes, we expect that onset, strength, and time course of anti-ACE2 IgG are sACE2 dose-dependent, with the lowest titers for subimmunogenic amounts of sACE2. Induction of autoimmunity through an sACE2:spike piggyback has also been suggested in a theoretical review by McMillan et al. [19]. To address if complex formation may drive ACE2 autoimmunity, we made use of our existing dataset to assess whether the levels of anti-ACE2 IgG in COVID-19 patient sera are associated with serum concentrations of sACE2 and observed a weak but significant correlation ($p = 1.3 \times 10^{-9}$, $R = 0.4$, Fig. 1G). However, the increased level of sACE2 does not temporally precede the emergence of anti-ACE2 IgG and decent titers were even observed for patients with the lowest levels of sACE2 (Fig. 1G; Supporting information Fig. S1C). Collectively, our data suggest that sACE2 is not the main driver eliciting anti-ACE2 IgG.

Anti-ACE2 autoantibodies in COVID-19 patients do not affect ACE2 enzymatic function

ACE2 is an important regulator of blood pressure and inflammation 12, 13. We previously found that in contrast to healthy donor samples, COVID-19 patient sera inhibit enzymatically active, recombinant ACE2, suggesting that ACE2-reactive IgG might inhibit the enzymatic activity. However, we observed that the level of ACE2-reactive IgG correlates weakly and negatively with inhibition of ACE2 by COVID-19 serum (Fig. 1H), suggesting that autoantibodies do not affect ACE2 regulatory functions. To formally exclude that patient immunoglobulins are capable of impairing ACE2 activity, we purified Ig from COVID-19 sera by protein G pull-down and determined the inhibitory potential of the eluate and the IgG-depleted fraction. The pull-down removed 99.97% of serum IgG (Supporting information Fig. S1D) but not the inhibitory potential of the depleted fraction (Fig. 1I). Conversely, purified Ig did not reduce the enzymatic activity of ACE2. To assess the concentration of polyclonal anti-ACE2 Ig that would be sufficient to inhibit ACE2 activity, we used a
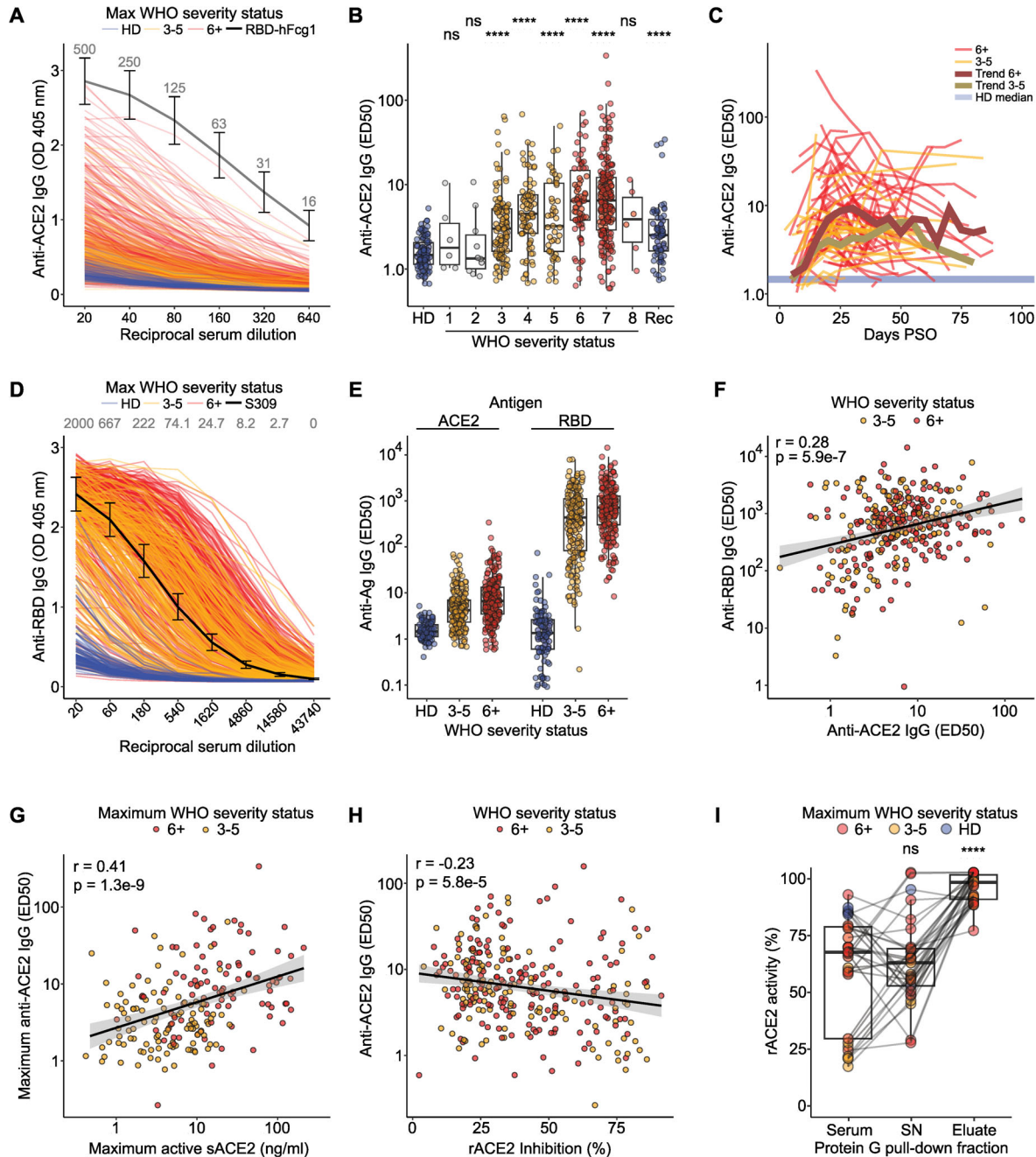
Figure 1. **ACE2-reactive IgG is significantly elevated in COVID-19 but insufficient for enzyme inhibition.** (A) ACE2-reactive IgG in sera of healthy donors in blue (HD, $n = 96$, one sample per donor), moderate COVID-19 in yellow (WHO3-5, $n = 107$ patients, $n = 210$ samples) and severe patients in red (WHO6+, $n = 94$ donors, $n = 370$ samples). Shown are the ELISA optical density (OD) values for indicated reciprocal serum dilutions. An RBD-hFcg1 control at indicated concentrations (gray numbers, ng/mL) was added to each plate ($n = 57$). (B) Normalized ED50 of anti-ACE2 IgG in COVID-19 patients and recovered (Rec) individuals. (C) Kinetics of anti-ACE2 IgG (ED50) with median trend over indicated days post symptom onset (PSO). (D) SARS-CoV-2 RBD-reactive IgG at indicated serum dilutions. The monoclonal antibody S309 (gray numbers, concentration in ng/mL) was added to each plate ($n = 68$) for standardization of the ED50. (E) ED50 values of ACE2- versus RBD-reactive IgG by COVID-19 severity class. (F) Spearman correlation of anti-RBD IgG and anti-ACE2 IgG in $n = 392$ serum samples drawn ≥ 15 days PSO from 133 donors. (G) Spearman correlation of maximal anti-ACE2 IgG (ED50) and maximal sACE2 serum concentrations that were detected in $n = 201$ COVID-19 patients. (H) Levels of anti-ACE2 IgG versus the capability of serum samples to inhibit the activity of recombinant ACE2 (rACE2) that was added at a final serum concentration of 50 ng/mL ($n = 300$ serum samples drawn ≥ 15 days PSO from 125 donors). Spearman correlation analysis in (F–H) and the curve fitting was performed with a 95% confidence interval. (I) The ACE2 inhibitory potential of whole serum was compared to protein G pull-down fractions. Severe (red, $n = 15$) and moderate (orange, $n = 10$) COVID-19 patient samples with high ($n = 8$) and low ($n = 17$) inhibitory potentials were compared to healthy donor sera (blue, $n = 4$). Combined data from four independent experiments, each sample was tested in six serial, single dilutions (A–H). For ACE2 activity and rACE2 inhibition, combined data from three experiments are represented, samples tested in a single dilution in two replicates (G–H). Data from a single experiment is represented in I, samples are tested in two replicates. Symbols represent individual samples, boxes show the median and the interquartile range, and the whiskers display 95% confidence interval. ****$p < 0.0001$; ns = no significance.

commercial polyclonal antibody with moderate binding affinity to human ACE2. To reduce ACE2 enzymatic activity by half, concentration of anti-ACE2 had to exceed 10 μg/mL (Supporting information Fig. S1E). Taken together, our data suggest that ACE2 inhibition in COVID-19 sera stems from an unknown factor as the levels of anti-ACE2 Ig are too low to impact ACE2 regulatory functions.

The majority of COVID-19 patients develop polyreactive serum IgG

As ACE2-reactive IgG was unlikely to stem from a target-driven response, we postulated that similar levels of autoreactivity might be detected for other serum proteins. We chose soluble CD26, also called dipeptidyl peptidase 4 (DPP4), as a control antigen, because it is an enzyme that circulates in sera of healthy individuals at levels similar to sACE2 in COVID-19 patient blood [20]. We observed a significant increase of autoreactivity against sDPP4 in COVID-19 patients, comparable to the autoreactivity against ACE2 (anti-ACE2 IgG ED50 median 5.35 vs. anti-DPP4 IgG ED50 median 8.47, including WHO1-8 class severities, Supporting information Fig. S2A and B). Similar to ACE2-reactive IgG, longitudinal measurement unraveled the highest level of anti-DPP4 IgG during the acute phase of the disease up to 50 days post symptom onset, with a gradual decline over 7 weeks (Fig. 2A).

The risk of severe illness upon SARS-CoV-2 infection is increased if pre-existing autoantibodies neutralize type I IFNs [1]. To compare levels of anti-DPP4 and anti-ACE2 reactive antibodies to functionally relevant autoimmune Ig in COVID-19, we measured antibodies recognizing IFNα2 (Supporting information Fig. S2C and D). As expected, COVID-19 patients displayed elevated levels of IFNα2 reactive antibodies, which peaked over the first month of the infection, similar to anti-ACE2 IgG (Fig. 2B). Of note, all tested self-reactivities were strongly and positively correlated, including antibodies recognizing bovine serum albumin (BSA) (ACE2 vs. BSA, $r = 0.89$; ACE2 vs. DPP4, $r = 0.88$; ACE2 vs. IFNα2, $r = 0.77$, $p < 0.0001$, Fig. 2C–F). These data suggest that the majority of COVID-19 sera display a promiscuous reactivity of serum IgG. Of note, only a small fraction of patient samples showed autoantibody titers for a particular self-antigen beyond the levels of polyreactivity (elevated ACE2-reactive IgG in $n = 8$ sera [5 donors], 1.3% of total samples [2.0% of total donors], elevated anti-IFNα2 IgG in $n = 18$ sera [10 donors], 2.8% of total samples [4.0% of total donors], with reactivity defined as ED50 $> 2 \times$ maximum healthy donor titer and specificity defined as the ratio of anti-ACE2/anti-IFNα2 IgG deviating by more than 1.5 $\times$ SD from the median ratio). While ACE2-reactive samples were not able to inhibit recombinant ACE2, IFNα2-specific samples displayed a moderate inhibitory potential (Supporting information Fig. S2E). Samples obtained from patients with systemic lupus erythematosus (SLE, 58 donors), displayed low levels of polyreactivity as indicated by low levels of ACE2 and BSA reactive IgG (Fig. 2G).

Polyreactive serum IgG in COVID-19 patients poorly compromises IFN signaling

Finally, we aimed to test the inhibitory potential of promiscuous versus target-reactive sera with similar titers of anti-IFNα2 IgG. We, therefore, selected $n = 7$ donors per group and applied published protocols [1] to determine STAT1 (signal transducers and activators of transcription 1) activation after stimulating healthy donor PBMCs (peripheral blood mononuclear cells) with 10 ng/mL IFNα2 in the presence of selected sera. Interestingly, we found that only one out of eight donors with polyreactive sera impaired STAT1 activation. By contrast, six out of seven donors with sera containing anti-IFNα2 IgG effectively blocked IFN signaling (Fig. 2H–J). To determine whether polyspecific sera may impair STAT1 signaling for lower concentrations of IFNα2, we selected a subset of promiscuous and IFNα2-reactive donor samples ($n = 3$ per group) and performed the experiments with IFNα2 concentrations ranging from 10 pg/mL to 10 ng/mL. For two out of three promiscuous samples, we observed a moderate drop in STAT1 phosphorylation in presence of 1 ng/mL IFNα2 in comparison to healthy donor control, while the IFNα2-reactive sera strongly inhibited the STAT1 activation in presence of any IFNα2 concentration (Supporting information Fig. S2F). In conclusion, our data suggest that compared to promiscuous autoantibodies, target-specific Ig is more likely to interfere with the function of the self-protein.

Concluding remarks

Collectively, our study highlights a relevant aspect at the intersection of autoimmunity and COVID-19, namely that SARS-CoV-2 infection is associated with high levels of polyreactive IgG that can confound the detection of target-specific and functionally relevant autoantibodies. Diverse autoantibodies were described to be associated with COVID-19. Confirming previous reports, we found that ACE2- and IFN-reactive IgG significantly correlate with COVID-19 disease severity. However, our findings argue that autoantibodies need to be evaluated in the context of multiple self-reactivities to discriminate promiscuous from target-specific autoimmunity. Such discrimination may be of particular relevance when guiding the prediction of disease course as well as therapeutic interventions. For instance, the capability of serum IgG to interfere with IFN activity may be carefully considered when applying therapies enhancing IFN-signaling, urging to prioritize functional assays over ordinary titer measurements for diagnostic testing. In fact, validation of ELISA assays by a competition assay has been suggested as part of a diagnostics pipeline to exclude anti-IFN-Ig false positives [21].

It has been shown in the past that a large proportion of memory B cells and serum antibodies in healthy donors display polyreactivity [22]. Therefore, the rise of IgG binding self-antigens after SARS-CoV-2 infection might be explained by the differentiation of polyreactive memory B cells into antibody-secreting plasma cells, giving rise to large amounts of IgG capable of binding
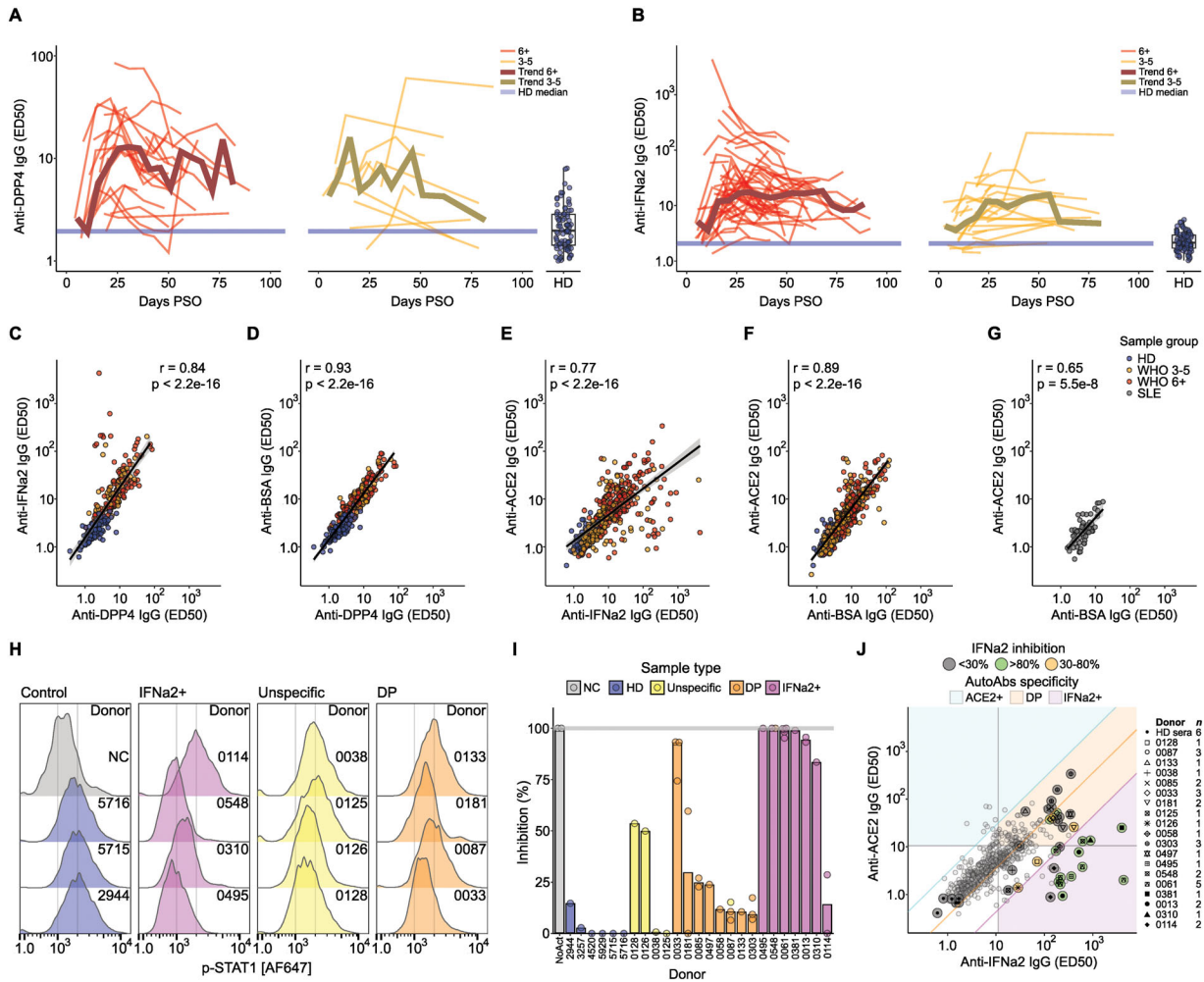
Figure 2. Serum IgGs of severe COVID-19 patients that are promiscuously self-reactive lack inhibition of cytokine function, while COVID-sera containing target-specific anti-IFNα2 IgG are inhibitory. (A) Anti-human DPP4 IgG at indicated days post symptom onset (PSO) for moderate and severe COVID-19 patients. Trendlines for median ED50 values are shown. (B) The ED50 of anti-IFNα2 IgG over time PSO. Boxplots for healthy donors (HD) in blue show median and the interquartile range, whiskers represent 95% confidence interval. (C) Spearman correlations showing ED50 values of anti-IFNα2 IgG versus anti-DPP4 IgG, (D) anti-BSA IgG versus anti-DPP4 IgG. In (C) and (D), $n = 188$ samples from 45 COVID-19 patients are shown. (E) Anti-ACE2 IgG versus anti-IFNα2 IgG ($n = 449$ samples from 150 COVID-19 patients); (F) anti-ACE2 IgG versus anti-BSA IgG for 429 serum samples of 168 COVID-19 patient donors. In (D–F), $n = 96$ samples from healthy donors are shown in blue. (G) Spearman correlations of anti-ACE2 IgG versus anti-BSA IgG of sera collected from $n = 58$ systemic lupus erythematosus (SLE) patients (one sample per donor). (H) The IFNα2 blocking activity was assessed by stimulating peripheral blood mononuclear cells (PBMCs) with 10 ng/mL IFNα2 in the presence or absence of 10% healthy control or patient serum. Fluorescence staining of phosphorylated (p-) STAT1 is depicted for an unstimulated control (gray), three healthy donors (blue), four donors with anti-IFNα2 IgG (IFNα2+, violet), four donors with unspecific IgG (unspecific, yellow), and four donors with promiscuous IgG (DP, orange). (I) Inhibitory potential was calculated as a relative decrease in p-STAT1 mean fluorescence intensity (MFI) in comparison to the level in absence of IFNα2 (NoAct, gray line) and in presence of healthy donor sera (HD, blue). Sample type was assigned based on the anti-IFNα2 and anti-ACE2 IgG level, criteria are illustrated in (J) and described in the text. Each point represents a sample, bar plot shows the median level for a donor. (J) The ED50 values of anti-ACE2 versus anti-IFNα2 IgG with the zones discriminating ACE2-specific (ACE2+, cyan fill), promiscuous (DP, orange fill), and IFNα2-reacive (IFNα2+, purple fill) sera, respectively. Orange line denotes the median ratio between anti-ACE2 and anti-IFNα2 IgG, cyan, and purple lines delineate median $\pm$ 1.5 $\times$ SD anti-ACE2/IFNα2 IgG, accordingly. Serum samples with less than 30% (gray), 30–80% (orange), and more than 80% (green) STAT1 phosphorylation inhibition are highlighted. Vertical and horizontal gray lines denote double of the maximum anti-IFNα2 and anti-ACE2 IgG titers for healthy donors, correspondingly. Combined data from three experiments are shown in (A) and (B); (C–G) the combined data from seven experiments are represented. In (A–G), each sample is tested in six dilutions in one replicate. For STAT1 phosphorylation assay, data from two independent experiments are combined, the samples are tested in a single dilution in two replicates (H–J).

multiple distinct targets promiscuously and with low affinity. In addition, certain viral infections were shown to promote polyreactivity including EBV, hepatitis viruses, and HIV [23]. Similarly, SARS-CoV-2 may drive the emergence of polyreactive serum antibodies.

Interestingly, polyreactivity was suggested to confer a selective advantage to virus-specific antibodies against HIV [24]. Owing to the exceptionally low number of spike proteins per virion [25], a binding mode called heteroligation would ensure bivalent binding of antibodies with one binding site attaching to the specific

target with high affinity, while the second site would bind a distinct molecular structure on HIV with low affinity [24]. As spike proteins on SARS-CoV-2 can be scarce [26], polyreactivity may similarly enhance antibody binding through an avidity gain. However, formal clarification demands the analysis of monoclonal SARS-CoV-2 spike-reactive antibodies for polyreactive properties.

Finally, the deep characterization of self-reactive antibodies, including their kinetics and longevities, may in future be expanded toward the definition of target-focused versus promiscuous reactivities to support clinical prognosis and inform the impact of autoantibodies on COVID-19 or long-COVID pathologies.

Materials and methods

Patient samples

A total of 640 samples were obtained from healthy donors and COVID-19 patients, recruited as outpatients (19 donors) or at hospitals (228 donors of the Pa-COVID-19 study cohort). Based on patient availability, single blood draws or longitudinal sampling up to 7 months post symptom onset was provided (146 patients of the Pa-COVID-19 study cohort). Patients included in this analysis were not vaccinated and recruited from March 4, 2020 until January 5, 2021. Treatment followed the standard of care throughout the study period with the administration of dexamethasone for patients requiring respiratory support from mid-June, 2020 according to the preliminary results of the RECOVERY trial [27, 28]. Some patients received prednisolone or equivalents of other glucocorticoids before the introduction of dexamethasone or as a substitute for dexamethasone for individual reasons. A healthy donor cohort enrolled SARS-CoV-2 negatively tested Charité healthcare workers (96 donors with single donations). COVID-19 severity states were categorized according to the WHO ordinal scale for clinical improvement: no clinical or virological evidence of infection (WHO0), ambulatory without limitation of activities (WHO1), ambulatory with limitations of activities (WHO2), hospitalized mild disease without oxygen therapy (WHO3), hospitalized mild disease with oxygen by mask or nasal prongs (WHO4), hospitalized severe disease with non-invasive ventilation or high-flow oxygen (WHO5), hospitalized severe disease with intubation and mechanical ventilation (WHO6), hospitalized severe disease with intubation, mechanical ventilation, and additional organ support—pressors, RRT, or ECMO (WHO7), death (WHO8). Outpatient subjects recovered from mild or moderate COVID-19 (WHO1-3) for at least 4 weeks before convalescent plasma donations. All samples were collected in compliance with the principles laid down in the 1964 Declaration of Helsinki and its later amendments. All patients gave written informed consent. Note that 68.9% of hospitalized COVID-19 patients were male. Female patients had a median age of 60 years (min.: 18; max.: 89 years) and a median BMI of 29.0 kg/m^2 (min.: 20; max.: 56 kg/m^2). Male patients had a median age of 61 years (min.:

21; max.: 92 years) and a median BMI of 27.8 kg/m^2 (min.: 16; max.: 54 kg/m^2). COVID-19 outpatients were 42% male and had a median age of 52 years (min.: 26, max.: 79 years). The healthy donor cohort was 54% male. Female donors had a median age of 43 years (min.: 23; max.: 83 years) and a median BMI of 22.6 kg/m^2 (min.: 17.4; max.: 33.7 kg/m^2). Male donors had a median age of 49 years (min.: 20; max.: 86 years) and a median BMI of 25.3 kg/m^2 (min.: 20.7; max.: 36.9 kg/m^2). A total of 58 samples (one sample per donor) were received from patients suffering from SLE. Patients included in this analysis were recruited from May, 2020 until May, 2021. SLE patients were diagnosed in accordance with the joint guidelines by the European League Against Rheumatism and the American College of Rheumatology [29]. All SLE patients tested positive for antinuclear antibodies. Note that 95% of SLE patients were female. Male SLE patients had a median age of 50 years (min.: 32, max.: 67 years). Female SLE patients had a median age of 38.5 (min.: 19, max.: 72 years).

Collection of sera and plasma

Sera were obtained from blood collected in tubes containing clot activator of silica particles, followed by centrifugation. Serum and plasma were stored at 4°C.

Cloning of recombinant protein

Q18-V739 fragment of human ACE2 (Uniprot: Q9BYF1, GeneID: 59272) was cloned into mammalian expression pcDNA3.1 vector containing a signal peptide (SP) and a molecular tag composed of eight histidine moieties (His-tag) connected to the C-terminus of ACE2 via GSSGSSGSS linker. It was determined experimentally that C-end His-tag is not suitable for efficient protein purification, likely due to the cleavage by proteases such as a disintegrin and metalloprotease 17 (ADAM17) expressed by 293 cells. Therefore, a His-tag was introduced between the SP and the N-terminus of the ACE2 fragment. An RBD expression vector was kindly provided by Krammer and colleagues [30]. R319-F541 fragment of Wuhan SARS-CoV-2 Spike was cloned upstream to CH2 and CH3 domains of human IgG1 to generate RBD-hFcg1. Human DPP4 fragment S39-P766 (Uniprot: P27487, GeneID: 1803) was cloned into mammalian expression pcDNA3.1 vector containing an SP and a molecular tag composed of eight histidine moieties (His-tag) connected to the N-terminus of DPP4. Human IFNα2 fragment C24-E188 (Uniprot: P01563, GeneID: 3440) was cloned into mammalian expression pcDNA3.1 vector containing an SP and a molecular tag composed of eight histidine moieties (His-tag) connected to the C-terminus of IFNα2 via GSSGSSGSS linker. Begelomab heavy and light chain variable domains (PubChem SID: 252166891) were assembled via overlap-extension PCR and cloned into pcDNA3.1 vector containing an SP and heavy and light chain constant domains. Monoclonal polyreactive IgG control was constructed by cloning the variable domain of heavy

chain-only antibody VHH J3 [31] flanked by GS-linkers and IgG1 hinge motifs (EPKSCDKTHTCPPCP) into the anti-influenza stem FY1 antibody [32] downstream to the variable domain. The heavy chain was paired with the cognate light chain of the FY1 antibody and expressed in FreeStyle 293-F cells (Life Technologies, #R79007) according to the procedure described below.

Production of recombinant proteins

Cloning constructs were used to transiently transfect FreeStyle 293-F cells that were grown in suspension using Expi293 expression medium (Life Technologies; #A1435101) at 37°C in a humidified 8% CO_2 incubator shaking at 120 rpm. Cells were grown to a density of 2.5 million cells per milliliter, transfected using polyethylenimine (PEI; Polysciences Europe GmbH; #23966-1) (4 μg/mL in cell suspension) and plasmid DNA (1.2 μg/mL in cell suspension) that were diluted in Opti-MEM (Gibco; #31985047) medium and cultivated for 3 days. The supernatants were harvested and proteins purified by His or Ab SpinTrap columns according to manufacturer's protocol (Cytiva; His: #28-9321-71; Ab: #28-4083-47). The eluted protein was buffer exchanged to PBS (Sigma-Aldrich; #D8537-500ML) using Amicon Ultra-4 ultrafiltration column with 10 kDa (Millipore, #UFC801096) or 100 kDa cutoff (Millipore, #UFC810008). Protein concentration was determined by a DS-11 spectrophotometer (DeNovix). Protein production was confirmed by Western blot.

ACE2 enzymatic activity measurement

Enzymatic activity of ACE2 was determined by cleavage of the fluorescent substrate Mca-Ala-Pro-Lys(Dnp) (Mca = (7-methoxycoumarin-4-yl)acetyl; Dnp = (2,4-dinitrophenyl), Carbosynth Limited, #FM111000), which quenches the Mca fluorescence (Max Absorption/Emission upon cleavage = 325/393 nm) until the Pro-Lys linker is cleaved [33]. The reaction was performed by mixing 7.5 μL serum (or protein G pull-down eluate) in 1:2–1:54 dilutions with 7.5 μL PBS-1% BSA (or, when ACE2-inhibitory capacity was measured, 7.5 μL 100 ng/mL rACE2-N'His) followed by the addition of 85 μL of substrate solution. For antibody-mediated inhibition measurement, RBD-hFcg1, goat anti-human ACE2 antibody (R&D Systems, #AF933), and goat anti-human IgG (Southern Biotech, #2040-01) were added at the indicated concentration. Substrate solution contained 8 μM Mca-Ala-Pro-Lys(Dnp) substrate, 75 mM trisaminomethane adjusted to pH 6.5 with hydrochloride, 1 M sodium chloride, 100 μM zinc chloride, and freshly added protease inhibitors: 10 μM Captopril (Sigma-Aldrich, #PHR1307), 10 μM bestatin hydrochloride (Sigma-Aldrich, #B8385), and 10 μM Z-Pro-prolinal (Sigma-Aldrich, #SML0205). All fluorescence measurements were performed using 340 nm excitation and 420 nm emission light filters (Cytation 5, BioTek). The sample baseline fluorescence (F340/420$_0$) and absorbance at 450 nm were determined imme-

diately after substrate addition, followed by incubation at 37°C in the dark. The second fluorescence measurement was performed after 1 h (F340/420). The concentration of active soluble ACE2 (a-sACE2) level was determined by interpolating the enzyme velocity (relative fluorescent units/time) of different amounts of self-made rACE2-N'His, calibrated with different commercial human recombinant ACE standards (Abcam, #ab151852; and Bon-Opus, #BP042) in the linear range of the calibration curve. Recombinant ACE2 was diluted to various concentrations from 0.01–100 ng/mL to obtain a calibration curve via linear regression with a zero-point intercept. All samples were measured in duplicates or in serial dilutions. The specificity of ACE2 substrate cleavage in serum and plasma was confirmed using the ACE2 selective inhibitor DX600 (Enzo LifeSciences GmbH, BV-9687-100). Sample storage and freezing did not alter ACE2 activity.

ELISA

Antigens were immobilized on a high-binding 96-well ELISA plate (Corning, #CLS3690) by incubating 25 μL of 10 μg/mL protein in PBS solution for at least 8 h at +4°C. After washing 3× with 100 μL/well PBS containing 0.05% of Tween-20 (PBST buffer), plates were blocked for 1 h with 100 μL/well 1% BSA in PBS (w/v), followed by 3× washing with 100 μL/well PBST. Sera were diluted in PBS-1% BSA to indicated serial dilutions, added to coated plates, and incubated for 1 h at room temperature. Distinct antibodies (S309, RBD-hFcg1, Begelomab, mPRIgG) were added at indicated concentrations. Plates were developed with an anti-human IgG-alkaline phosphatase (AP)-coupled antibody (SouthernBiotech #2040-04) diluted 1:500 in PBS 1% BSA. Bicarbonate buffer with 4-nitrophenyl phosphate disodium salt hexahydrate substrate (Sigma-Aldrich, #S0942-50TAB; 1 tablet per 20 mL buffer) was added (50 μL/well) and absorbance was measured at 405 nm after 30 min in a Cytation 5 device (BioTek). SARS-CoV-2 RBD fused to the Fc portion of human IgG1 (RBD-Fcg1) at distinct concentrations served as a reference to calculate a proxy for the amount of ACE2 autoantibodies in serum that corresponds to the RBD-Fcg1 ACE2 interaction. Note that 50% of maximum IgG binding (ED50) was determined by sigmoid curve fitting with nonlinear regression performed in R (stats package).

Protein G pull-down

Antibodies from patients' sera were pulled down by Pierce Protein G magnetic beads (Thermo Scientific, #88848) according to the manufacturer's instructions. Briefly, 50 μL serum was used to resuspend the beads washed in Tris buffer containing 0.1% Tween 20. After 1-h incubation on the shaker at RT, the beads were washed three times in Tris-Tween buffer and resuspended in 42 μL of 0.1 M Gly-HCl (pH 2.0) for 10 min. The eluate was collected in a separate tube and neutralized by one-sixth volume of 1

M Tris-HCl (pH 8.0). The successful pull-down was confirmed by absorbance measurement at 280 nm by a DS-11 spectrophotometer (DeNovix).

STAT1 phosphorylation analysis

PBMCs were extracted via Ficoll centrifugation and immediately used for activation. Note that 0.5 million cells were incubated with 10 ng/mL recombinant human IFNα2 in presence of 10% sera samples for 15 min at 37°C in RPMI complete medium. The activated cells were fixed with 1.5% formaldehyde for 10 min at room temperature, washed in PBS, permeabilized with 100% methanol for 20 min on ice, washed in PBS, and stained with 5 µg/mL p-STAT1 antibody (Y701, R&D Systems, AF2894) diluted in PBS + 10% FBS + 2 mM EDTA. After 20 min of staining, cells were washed twice in PBS-FBS-EDTA and stained with donkey anti-rabbit IgG conjugated with AlexaFluor-647 (Jackson ImmunoResearch, #711-605-152). Cells were washed twice in PBS-FBS-EDTA and analyzed in BD Fortessa. The MFI of forward/side-scatter pre-gated cells was calculated with FlowJo v10.8.1 software (BD Biosciences).

Statistics

Tests were two-tailed, and a *p*-value lower than 0.05 was considered statistically significant. A Shapiro–Wilk test was used for normality testing of continuous variables. An independent *t*-test was used when continuous data met the criteria of the normality test. Otherwise, the Mann–Whitney *U* test was used. Spearman correlations were performed with a 95% confidence interval.

References

1 Bastard, P., Rosen, L. B., Zhang, Q., Michailidis, E., Hoffmann, H. H., Zhang, Y., Dorgham, K. et al., Autoantibodies against type I IFNs in patients with life-threatening COVID-19. *Science* 2020. **370**: eabd4585.

2 Zuo, Y., Estes, S. K., Ali, R. A., Gandhi, A. A., Yalavarthi, S., Shi, H., Sule, G. et al., Prothrombotic autoantibodies in serum from patients hospitalized with COVID-19. *Sci. Transl. Med.* 2020. **12**: eabd3876.

3 Xiao, M., Zhang, Y., Zhang, S., Qin, X., Xia, P., Cao, W., Jiang, W. et al., Antiphospholipid antibodies in critically ill patients with COVID-19. *Arthritis Rheumatol.* 2020. **72**: 1998–2004.

4 Blagova, O., Varionchik, N., Zaidenov, V., Savina, P. and Sarkisova, N., Anti-heart antibodies levels and their correlation with clinical symptoms and outcomes in patients with confirmed or suspected diagnosis COVID-19. *Eur. J. Immunol.* 2021. **51**: 893–902.

5 Wang, E. Y., Mao, T., Klein, J., Dai, Y., Huck, J. D., Jaycox, J. R., Liu, F. et al., Diverse functional autoantibodies in patients with COVID-19. *Nature* 2021. **595**: 283–288.

6 Chang, S. E., Feng, A., Meng, W., Apostolidis, S. A., Mack, E., Artandi, M., Barman, L. et al., New-onset IgG autoantibodies in hospitalized patients with COVID-19. *Nat. Commun.* 2021. **12**: 5417.

7 Dotan, A., Muller, S., Kanduc, D., David, P., Halpert, G. and Shoenfeld Y., The SARS-CoV-2 as an instrumental trigger of autoimmunity. *Autoimmun. Rev.* 2021. **20**: 102792

8 Lan, J., Ge, J., Yu, J., Shan, S., Zhou, H., Fan, S., Zhang, Q. et al., Structure of the SARS-CoV-2 spike receptor-binding domain bound to the ACE2 receptor. *Nature*. 2020. **581**: 215–220.

9 Arthur, J. M., Forrest, J. C., Boehme, K. W., Kennedy, J. L., Owens, S., Herzog, C., Liu, J. et al., Development of ACE2 autoantibodies after SARS-CoV-2 infection. *PLoS One*. 2021. **16**: e0257016.

10 Rodriguez-Perez, A. I., Labandeira, C. M., Pedrosa, M. A., Valenzuela, R., Suarez-Quintanilla, J. A., Cortes-Ayaso, M., Mayán-Conesa, P. et al., Autoantibodies against ACE2 and angiotensin type-1 receptors increase severity of COVID-19. *J. Autoimmun*. 2021. **122**: 102683

11 Casciola-Rosen, L., Thiemann, D. R., Andrade, F., Trejo-Zambrano, M. I., Leonard, E. K., Spangler, J. B., Skinner, N. E. et al., IgM anti-ACE2 autoantibodies in severe COVID-19 activate complement and perturb vascular endothelial function. *JCI Insight*. 2022. **7**: e158362.

12 Donoghue, M., Hsieh, F., Baronas, E., Godbout, K., Gosselin, M., Stagliano, N., Donovan, M. et al., A novel angiotensin-converting enzyme–related carboxypeptidase (ACE2) converts angiotensin I to angiotensin 1–9. *Circ. Res*. 2000. **87**: E1–E9.

13 Benigni, A., Cassis, P. and Remuzzi, G., Angiotensin II revisited: new roles in inflammation, immunology and aging. *EMBO Mol. Med*. 2010. **2**: 247–257.

14 Imai, Y., Kuba, K., Rao, S., Huan, Y., Guo, F., Guan, B., Yang, P. et al., Angiotensin-converting enzyme 2 protects from severe acute lung failure. *Nature* 2005. **436**: 112–116.

15 Lambert, D. W., Yarski, M., Warner, F. J., Thornhill, P., Parkin, E. T., Smith, A. I., Hooper, N. M. et al., Tumor necrosis factor-alpha convertase (ADAM17) mediates regulated ectodomain shedding of the severe-acute respiratory syndrome-coronavirus (SARS-CoV) receptor, angiotensin-converting enzyme-2 (ACE2). *J. Biol. Chem*. 2005. **280**: 30113–30119.

16 Shulla, A., Heald-Sargent, T., Subramanya, G., Zhao, J., Perlman, S. and Gallagher, T., A transmembrane serine protease is linked to the severe acute respiratory syndrome coronavirus receptor and activates virus entry. *J. Virol*. 2010. **85**: 873–882.

17 Fagyas, M., Fejes, Z., Sütő, R., Nagy, Z., Székely, B., Pócsi, M., Ivády, G. et al., Circulating ACE2 activity predicts mortality and disease severity in hospitalized COVID-19 patients. *Int. J. Infect. Dis*. 2022. **115**: 8–16.

18 WHO. WHO R&D blueprint novel coronavirus COVID-19 Therapeutic Trial Synopsis 2020a. https://www.who.int/blueprint/priority-diseases/key-action/COVID-19_Treatment_Trial_Design_Master_Protocol_synopsis_Final_18022020.

19 McMillan, P., Dexhiemer, T., Neubig, R. R. and Uhal, B. D., COVID-19—a theory of autoimmunity against ACE-2 explained. *Front Immunol*. 2021. **12**: 582166.

20 Alkharsah, K. R., Aljaroodi, S. A., Rahman, J. U., Alnafie, A. N., Dossary, R. A., Aljindan, R. Y., Alnimr, A. M. et al., Low levels of soluble DPP4 among Saudis may have constituted a risk factor for MERS endemicity. *PLoS One*. 2022. **17**: e0266603.

21 Akbil, B., Meyer, T., Stubbemann, P., Thibeault, C., Staudacher, O., Niemeyer, D., Jansen, J. et al., Early and rapid identification of COVID-19 patients with neutralizing type I interferon auto-antibodies. *J. Clin. Immunol*. 2022. **42**: 1111–1129.

22 Tiller, T., Tsuiji, M., Yurasov, S., Velinzon, K., Nussenzweig, M. C., Wardemann, H., Autoreactivity in human IgG+ memory B cells. *Immunity* 2007. **26**: 205–213.

23 Mouquet, H. and Nussenzweig, M. C., Polyreactive antibodies in adaptive immune responses to viruses. *Cell. Mol. Life Sci*. 2012. **69**: 1435–1445.

24 Mouquet, H., Scheid, J. F., Zoller, M. J., Krogsgaard, M., Ott, R. G., Shukair, S., Artyomov, M. N. et al., Polyreactivity increases the apparent affinity of anti-HIV antibodies by heteroligation. *Nature* 2010. **467**: 591–595.

25 Stano, A., Leaman, D. P., Kim, A. S., Zhang, L., Autin, L., Ingale, J., Gift, S. K. et al., Dense array of spikes on HIV-1 virion particles. *J. Virol*. 2017. **91**: e00415- e00417.

26 Ke, Z., Oton, J., Qu, K., Cortese, M., Zila, V., McKeane, L., Nakane, T. et al., Structures and distributions of SARS-CoV-2 spike proteins on intact virions. *Nature* 2020. **588**: 498–502.

27 Kurth, F., Roennefarth, M., Thibeault, C., Corman, V. M., Müller-Redetzky, H., Mittermaier, M., Ruwwe-Glösenkamp, C. et al., Studying the pathophysiology of coronavirus disease 2019: a protocol for the Berlin prospective COVID-19 patient cohort (Pa-COVID-19). *Infection* 2020. **48**: 619–626.

28 Group, R. C., Horby, P., Lim, W. S., Emberson, J. R., Mafham, M., Bell, J. L., Linsell, L. et al., Dexamethasone in hospitalized patients with Covid-19. *N. Engl. J. Med*. 2020. **384**: 693–704.

29 Aringer, M., Costenbader, K., Daikh, D., Brinks, R., Mosca, M., Ramsey-Goldman, R., Smolen, J. S. et al., 2019 European League against Rheumatism/American College of Rheumatology classification criteria for systemic lupus erythematosus. *Arthritis Rheumatol*. 2019. **71**: 1400–1412.

30 Amanat, F., Stadlbauer, D., Strohmeier, S., Nguyen, T. H. O., Chromikova, V., McMahon, M., Jiang, K. et al., A serological assay to detect SARS-CoV-2 seroconversion in humans. *Nat. Med*. 2020. **26**: 1033–1036.

31 McCoy, L. E., Quigley, A. F., Strokappe, N. M., Bulmer-Thomas, B., Seaman, M. S., Mortier, D., Rutten, L. et al., Potent and broad neutralization of HIV-1 by a llama antibody elicited by immunization. *J. Exp. Med*. 2012. **209**: 1091–1103.

32 Kallewaard, N. L., Corti, D., Collins, P. J., Neu, U., McAuliffe, J. M., Benjamin, E., Wachter-Rosati, L. et al., Structure and function analysis of an antibody recognizing all influenza A subtypes. *Cell* 2016. **166**: 596–608.

33 Xiao, F. and Burns, K. D., Measurement of angiotensin converting enzyme 2 activity in biological fluid (ACE2). *Hypertension* 2017. **1527**: 101–115.

Abbreviations: **COVID-19**: coronavirus disease 2019 · **SARS-CoV-2**: severe acute respiratory syndrome coronavirus 2 · **ACE2**: angiotensin-converting enzyme 2 · **sACE2**: soluble ACE2 · **WHO**: World Health Organization · **ED50**: effective dilution 50 · **DPP4**: dipeptidyl peptidase 4 · **PSO**: post-symptom onset · **SLE**: systemic lupus erythematosus

Full correspondence: Prof. Kathrin de la Rosa, Berlin Institute of Health at Charité, Max Delbrück Center for Molecular Medicine in the Helmholtz Association, 13125 Berlin, Germany
e-mail: Kathrin.delaRosa@mdc-berlin.de